Proceedings of the Seventeenth International Conference on
Civil, Structural and Environmental Engineering Computing
Edited by: P. Iványi, J. Kruis and B.H.V. Topping
Civil-Comp Conferences, Volume 6, Paper 6.5
Civil-Comp Press, Edinburgh, United Kingdom, 2023
doi: 10.4203/ccc.6.6.5

Funicular analysis of symmetric arches with finite friction accounting for stereotomy

D. Aita, M. Bruggi and A. Taliercio

**Department of Civil and Environmental Engineering,
Politecnico di Milano, Milano, Italy**

Abstract

In this contribution the funicular analysis of symmetric masonry arches is performed by accounting for stereotomy, as well as for the presence of Coulomb's friction at the interfaces between the voussoirs. The classical thrust network analysis approach is then enhanced by removing the hypothesis that the friction coefficient is infinite. The procedure presented here handles networks with any topology, fixed plane projection and loads applied at the nodes, whose equilibrium conditions are managed by exploiting the force density method. At each joint, a set of local constraints is enforced to restrain the shear-to-normal component ratio of the force between two adjacent voussoirs. The minimization/maximization of the horizontal thrusts, formulated in terms of applicate of the restrained nodes, is achieved by solving the corresponding multi-constrained minimization/maximization problem through sequential convex programming. The results obtained via this funicular method are validated by means of a graphical procedure based on the lower bound theorem of limit analysis, known as Durand-Claye method, by considering a masonry arch with non-conventional stereotomy.

Keywords: limit analysis, stereotomy, masonry arches, Coulomb's friction, mathematical programming

1 Introduction

The Thrust Network (TN) analysis method was originally proposed by Block and coworkers [1, 2] as a new methodology for generating surfaces and networks subjected only to compressive forces. The procedure proposed here consists in a constrained force density method for the funicular analysis of vaulted masonry structures, within the theoretical framework of limit analysis. Starting from the algorithm proposed in [3], it aims at enriching the TN approach by removing the simplifying hypothesis of infinite friction coefficient proposed by Heyman [4]. Since friction is assumed to be finite of nil, the funicular analysis is achieved by considering the influence of the real stereotomy of the *voussoirs* on the stability of masonry vaults. As recalled by Aita [5], the effect of stereotomy on sliding equilibrium has been considered since the pre-elastic research on the mechanical behaviour of masonry arches. Indeed, as far as the XVIII century, Coulomb [6] studied the effect of the joint inclination on the equilibrium of a masonry arch with prescribed intrados and extrados. He provided the explicit solution in the case of a flat arch: if the straight lines on which the joints lie meet at a common point, sliding between the voussoirs cannot occur. Recently, this classical problem has been revisited by some scholars in order to find analytical or numerical solutions for triangular arches [7, 8, 9] and arches of different shapes [5].

Under Heyman's hypothesis of infinite friction [4], stereotomy was taken into account in [10] and [11]. These contributions aimed at studying the collapse conditions of semicircular and elliptical arches and showed that stereotomy affects the shape of the thrust line as well as the value of the limit minimum thickness, i.e., the thickness corresponding to the formation of a rotational mechanism.

Conversely, in [12] sliding is allowed, and the minimum thickness analysis of circular and elliptical masonry arches is conducted by re-interpreting the effect of finite friction as a geometric constraint on stereotomy. Finally, the research reported in [13, 14] aims at refining the three-dimensional thrust network analysis by considering not only the equilibrium conditions at the nodes, but also strength criteria at the joints that take friction into account. From the studies quoted above, the effect of stereotomy on the stability of arches turns out to be significant when friction is assumed to be finite, and mixed or sliding collapse modes can occur.

Due to the finite friction, however, a subtle issue arises from the mechanical point of view: the material is characterized by *non-standard* plastic behaviour, and the ensuing non-associated flow rule invalidates Heyman's *safe theorem* [4] for assessing the stability of the structure. A survey of the scientific literature on this subject is beyond the scope of the current paper. Without claiming completeness, it is remarked that it possible to identify some classes of problems for which the static theorem of limit analysis can be exploited to determine safe stress states [15]. Symmetric arches with non-conventional stereotomy belong to this class of problems: they are dealt with in this paper by means of the funicular method, and the results are validated through a modern re-visitation [16] of Durand-Claye's method [17, 18].

2 Funicular polygons of min/max thrust using the force density method and mathematical programming

2.1 Force density method

The "force density method" [19] is used to handle the equilibrium of funicular polygons. A polygon is made of m branches, which undergo axial forces only, and $n_s = n + n_f$ nodes. The horizontal and vertical axes of the Cartesian reference system with origin O are denoted by x and z, respectively. The arrays $\mathbf{x}_s$ and $\mathbf{z}_s$ collect the coordinates of the n_s nodes: $\mathbf{x}_f$ and $\mathbf{z}_f$ collect those of the n_f restrained nodes, where reactions arise, whereas $\mathbf{x}$ and $\mathbf{z}$ refer to the n unrestrained nodes, i.e. those subject to external loads. Let $\mathbf{C}_s$ be the matrix that defines the connectivity of the grid: it can be split into a submatrix $\mathbf{C}_f$, referring to the restrained nodes, and another, $\mathbf{C}$, addressing the unrestrained nodes. Denoting by $\mathbf{u}$ and $\mathbf{w}$ the arrays that gather the difference in the coordinates of the nodes at the ends of each branch along the axis x and z, respectively, one has:

$$\mathbf{u} = \mathbf{C}_s \mathbf{x}_s, \quad \mathbf{w} = \mathbf{C}_s \mathbf{z}_s. \tag{1}$$

The force density vector $\mathbf{q} = \mathbf{L}^{-1}\mathbf{s}$ collects the force-to-length ratio for each branch of the funicular polygon, being $\mathbf{s}$ the array that collects the forces in the m branches. The lengths of the branches, $l_i = \sqrt{u_i^2 + w_i^2}$, are stored in an array $\mathbf{l}$, while $\mathbf{L} = \mathrm{diag}(\mathbf{l})$. In this study, only gravity loads are considered. Vertical point forces are prescribed at the unrestrained nodes through vector $\mathbf{p}_z$. Because of the introduction of the force density vector, the equilibrium of the unrestrained nodes can be expressed by means of linear equations that are uncoupled in the two considered directions. As reported in [2, 20, 21], in funicular polygons and networks with fixed plane projection an independent set of force densities can be identified. Indeed, the horizontal equilibrium of the loaded nodes of the funicular polygon reads:

$$\mathbf{C}_s \mathbf{x}_{s0}\, \mathbf{q} = \mathbf{0}, \tag{2}$$

where $\mathbf{x}_{s0}$ collects the fixed x coordinate of the nodes. Eqn. (2) implies that $m - r$ independent force densities $\overline{\mathbf{q}}$ can be retrieved, being r the rank of the coefficient matrix. The r dependent force densities $\widetilde{\mathbf{q}}$ can be expressed as:

$$\widetilde{\mathbf{q}} = \mathbf{B}\overline{\mathbf{q}} + \mathbf{d}, \tag{3}$$

where $\mathbf{B}$ and $\mathbf{d}$ are matrices whose constant entries can be derived by applying Gauss-Jordan elimination to Eqn. (2), see [22]. Upon introduction of $\mathbf{Q} = \mathrm{diag}(\mathbf{q})$, the equilibrium along the z axis reads:

$$\mathbf{C}^T \mathbf{Q} \mathbf{C} \mathbf{z} + \mathbf{C}^T \mathbf{Q} \mathbf{C}_f \mathbf{z}_f = \mathbf{p}_z. \tag{4}$$

The above equation is solved to compute the vertical coordinates of the unrestrained nodes of the funicular polygon. It is finally remarked that, due to symmetry, only one independent force density exists in the investigated problems, denoted by $\overline{q}$ hereafter.

2.2 Forces and eccentricities at the joints

Consider the i-th joint between any two adjacent voussoirs: let C_i be the centroid of the rectangular section and P_i the point where the line of action of the funicular force $\mathbf{F}_i$ crosses the joint (or "center of pressure"). Also, let $\boldsymbol{\xi}_i$ and $\boldsymbol{\eta}_i$ be the principal axes of inertia of the section, with $\boldsymbol{\eta}_i$ lying in the (x, z)-plane. The normal to the joint is denoted by $\mathbf{n}_i$. The section has size $l_{i,\xi} \times l_{i,\eta}$.

Denoting by $\mathbf{e}_x$ and $\mathbf{e}_z$ the unit vectors aligned with x and z, respectively, one has:

$$\mathbf{F}_i = s_i \left(\frac{u_i}{l_i} \mathbf{e}_x + \frac{w_i}{l_i} \mathbf{e}_z \right) = q_i \left(u_i \, \mathbf{e}_x + w_i \, \mathbf{e}_z \right). \tag{5}$$

Denoting by $\mathbf{N}_i$ the normal component of $\mathbf{F}_i$, its magnitude may be straightforwardly found as $N_i = \mathbf{F}_i \cdot \mathbf{n}_i$. Its eccentricity with respect to $\boldsymbol{\xi}_i$ can be computed by evaluating the moment of $\mathbf{N}_i$ about the same axis, $M_{i,\xi}$, scaled by N_i. Recalling that the shear component of the force $\mathbf{F}_i$ does not provide any contribution to $M_{i,\xi}$, one may conveniently compute:

$$e_{i,\xi} = \text{abs} \left(\frac{M_{i,\xi}}{N_i} \right), \text{with} \;\; \frac{M_{i,\xi}}{N_i} = \frac{\boldsymbol{\xi}_i \cdot (\mathbf{r}_i \times \mathbf{F}_i)}{N_i}, \tag{6}$$

where $\text{abs}(\cdot)$ stands for the absolute value of the scalar argument, and $\mathbf{r}_i$ is the vector drawn from C_i to any point belonging to the line of action of $\mathbf{F}_i$ (in particular, any of the vertices of the funicular polygon lying in the two adjacent voussoirs).

The magnitude of the shear component V_i can be found as the modulus of the vector difference $\mathbf{F}_i - \mathbf{N}_i$, i.e. $V_i = \mathbf{F}_i - N_i \mathbf{n}_i$.

2.3 Optimization problem

Within the framework of limit analysis, it is useful to investigate the range of admissible solutions, looking for both the minimum and maximum thrust in the arch. Hence, the following problem is addressed:

$$\begin{cases} \min\limits_{\substack{\overline{q} \leq 0 \\ \mathbf{z}_f^{min} \leq \mathbf{z}_f \leq \mathbf{z}_f^{max}}} \quad f = \pm R_h & \text{(7a)} \\ \text{s.t. } \widetilde{\mathbf{q}} = \mathbf{B}\overline{q} + \mathbf{d}, & \text{(7b)} \\ \mathbf{C}^T \mathbf{Q} \mathbf{C} \mathbf{z} + \mathbf{C}^T \mathbf{Q} \mathbf{C}_f \mathbf{z}_f = \mathbf{p}_z, & \text{(7c)} \\ \left(\dfrac{N_i}{\sigma_c \left(l_{i,\eta} - 2e_{i,\xi} \right) l_{i,\xi}} \right)^2 \leq 1 \quad \text{for } \; i = 1...m, & \text{(7d)} \\ \left(\dfrac{V_i}{N_i \tan \psi} \right)^2 \leq 1 \quad \text{for } \; i = 1...m. & \text{(7e)} \end{cases}$$

In the objective function 7a, R_h is the magnitude of the horizontal reaction (along x) at any of the two restrained nodes of the arch. The minimization unknowns are the

independent force density $\overline{q}$ and the applicates of the restrained nodes $\mathbf{z}_f$. The dependent force densities $\widetilde{\mathbf{q}}$ are computed from the independent one by means of Eqn. (7b), whereas Eqn. (7c) enforces the equilibrium of the unrestrained nodes in the vertical direction. The occurrence of any positive independent force density is prevented by the side constraint on $\overline{q}$. Side constraints on $\mathbf{z}_f$ prescribe lower and upper bounds to the vertical coordinates of the n_f restrained nodes, denoted by $\mathbf{z}_f^{min}$ and $\mathbf{z}_f^{max}$, respectively. Denoting by $\sigma_c \leq 0$ the compressive strength, Eqn. (7d) is used to prevent crushing at the i-th no-tension joint. A uniform distribution of compressive stresses is assumed to occur at a limited portion of the section of each joint, i.e. the area of size $(l_{i,\eta} - 2e_{i,\xi}) \times l_{i,\xi}$, see in particular [13] and [23]. Upon introduction of the friction angle ψ, the set of local enforcements in Eqn. (7e) imposes that the ratio V_i to N_i must obey the Coulomb's law [6]. Setting $\sigma_c \to -\infty$ in Eqn. (7d) and neglecting Eqn. (7e), the formulation in Eqn. (7) searches for networks of minimum/maximum thrust according to Heyman's assumptions.

As shown in [3], the problem in Eqn. (7) can be effectively solved by adopting techniques of sequential convex programming that were originally conceived to handle size optimization problems. In this contribution the gradient-based Method of Moving Asymptotes (MMA) [24] is adopted.

3 The stability area method

In order to validate the funicular approach described in Section 2, a historical method, based on the static theorem of limit analysis, is adopted [17, 18], by referring to the modern re-visitation proposed by Aita, Barsotti and Bennati [16, 23]. For symmetric, symmetrically loaded arches, the procedure allows one to visualize the domain of the admissible solutions by drawing the so-called *area of stability* in the (f, e_0) plane (Figure 1a), where f is the horizontal thrust acting at the ideal vertical crown section, while e_0 identifies the position of the centre of pressure at the crown, i.e., the eccentricity of f with respect to the cross section's centroid. The equilibrium of the portion of arch comprised between the ideal vertical crown section and any joint i (Figure 1b) can be formally written by taking into account the internal reactions at i. Thus, the normal force, N_i, and the bending moment, $M_{i,\xi}$, can be expressed as $M_{i,\xi}(f, e_0, \theta_i)$, $N_i = N_i(f, \theta_i)$, where θ_i is the inclination of the i-th joint with respect to the z axis. Under the hypotheses of infinite compressive strength and nil tensile strength, the limit bending moment, $M_{i,\xi}^{lim}$, is given by $M_{i,\xi}^{lim} = \text{abs}(N_i\, l_{i,\eta}/2)$.

With reference to Figure 1a, the inequalities $-M_{i,\xi}^{lim} \leq M_{i,\xi} \leq +M_{i,\xi}^{lim}$ implicitly define the region A_i^{rot} in the (f, e_0) plane, corresponding to the rotational domain related to the i-th joint (see the grey region). The procedure must be repeated for all the joints i; the intersection between all the areas A_i^{rot} provides the rotational domain related to the entire arch, A^{rot}, that is the yellow region in Figure 1a. If friction is assumed to be finite, the limit values of the crown thrust as regards sliding, $f_{i,min}^{sl}$ and $f_{i,max}^{sl}$, can be determined. The translational equilibrium of the considered arch portion can be enforced graphically (Figure 1b). Let W_i be the weight of this portion:

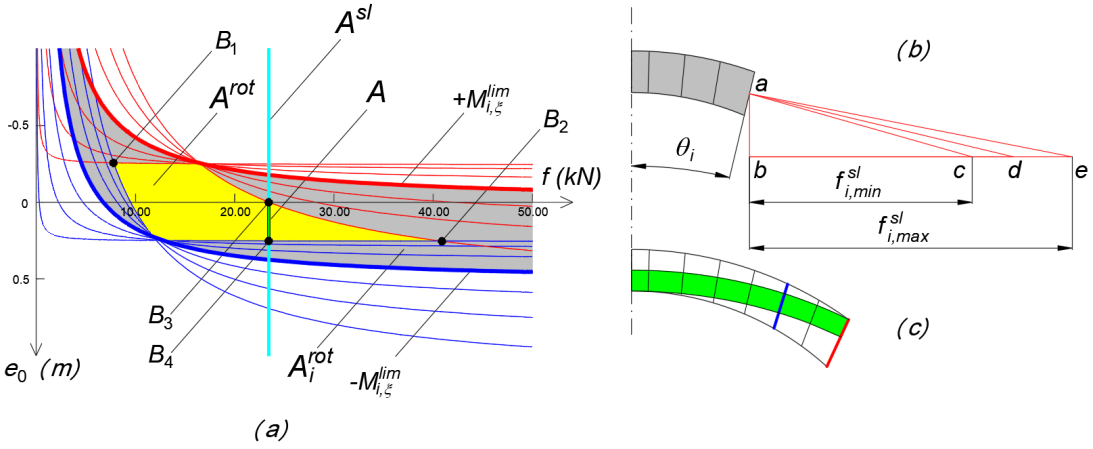

Figure 1: (a) stability area; (b) graphical construction to determine $f^{sl}_{i,min}$ and $f^{sl}_{i,max}$; (c) thrust lines corresponding to the limit friction coefficient, $\tan\psi = 0.0004915$.

at each joint i, by starting from any point a belonging to the joint, a vertical segment ab representing the magnitude of W_i is drawn to the same scale as that adopted in Figure 1a for the horizontal crown thrust, f. Then, the straight lines ac, ae, are traced so that they form an angle ψ with the straight-line ad perpendicular to joint i. The minimum and maximum values of the crown thrusts, $f^{sl}_{i,min}$, $f^{sl}_{i,max}$, are represented by segments bc, be. At these values of the crown thrust, the direction of the internal reaction at joint i is defined by the straight lines ac, ae, tangent to the friction cone. The graphical construction corresponds to the following analytical relations:

$$f^{sl}_{i,min} = W_i \tan\left(\pi/2 - \theta_i - \psi\right), \quad f^{sl}_{i,max} = W_i \tan\left(\pi/2 - \theta_i + \psi\right). \tag{8}$$

For each joint i, the inequalities $f^{sl}_{i,min} \leq f \leq f^{sl}_{i,max}$ identify the corresponding sliding domain A^{sl}_i in the (f, e_0) plane, comprised between two vertical straight lines (parallel to the e_0-axis). By intersecting all the regions A^{sl}_i, the sliding domain A^{sl} is obtained for the entire arch. In turn, the intersection between the rotational and sliding domains, A^{rot} and A^{sl}, provides the stability A. When the stability area related to the entire arch is reduced to a single point or a single segment, the limit condition is attained, and the corresponding collapse mechanism is identified. In Figure 1a, a limit condition is shown: the sliding domain A^{sl} corresponds to the cyan straight-line, while the stability area A shrinks to the green segment B_3B_4, which defines an infinite set of limit solutions (f, e_0). These solutions identify a unique value of the crown thrust, and a range of values for e_0. The admissible thrust lines are then comprised within the green region in Figure 1c, delimited by the thrust lines corresponding to points B_3 and B_4 of the stability area. For each of these solutions, an incipient collapse condition by pure sliding is identified: the arch portion above the blue joint slides inwards, while that comprised between the blue and red joint slides outwards (see Figure 1c).

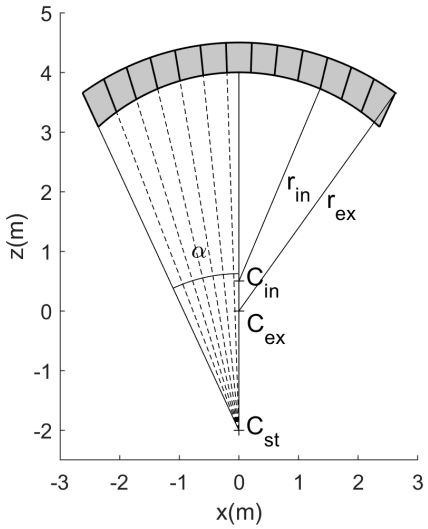

Figure 2: geometry and stereotomy of an arch.

4 A benchmark case study

A circular arch is addressed under self-weight, see Figure 2. The intrados lies along a circle with center at $C_{in} = (0, 0, 0.5)$ m and radius $r_{in} = 3.5$ m. The extrados lies along a circle having center at $C_{ex} = (0, 0, 0)$ m and radius $r_{ex} = 4.5$. One half of the angle of embrace is $\alpha = 24.88°$. A material with unit weight $\gamma_m = 15$ kN/m^3 is considered. The arch is made of thirteen voussoirs, whose stereotomy is defined by radial lines originating from the point $C_{st} = (0, 0, -2)$ m. The out-of-plane thickness is 0.5 m.

In Figure 3, the funicular networks of minimum and maximum thrust found for an infinite value of the compressive strength (for numerical purposes, σ_c was set equal to -1000 MPa) and infinite friction are shown, along with the forces in the branches of the network (in kN). The symbols $\circ$ and $+$ identify joints whose crossing branches activate a constraint related to the limit bending moment, see Eqn. (7d). The former symbol is used when the branch intersects the cross-section of the joint below the centroid; the latter, otherwise. In Figure 4, the funicular networks of minimum and maximum thrust found for the same value of σ_c, along with $\tan\psi = 0.0004915$, are represented. The symbol $\times$ refers to any joint whose crossing branch activates a friction constraint, see Eqn. (7e). Note that, in both pictures of figure 4, the shape of the funicular polygon and the relevant horizontal reaction R_h are the same, both for the maximum and the minimum thrust solution.

The results found with the funicular method are in full agreement with those obtained by means of Durand-Claye's method. In Figure 1a, the stability area is plotted for the considered arch. By assuming an infinite friction coefficient, the extreme values of the crown thrust are identified by the abscissas of points B_1 and B_2, $f_{min} = 7.789$ kN, $f_{max} = 40.886$ kN (Figure 1a). The arch is stable, since the stability area is a non-vanishing region of the $(f, e_0)-$plane. Giving the fric-

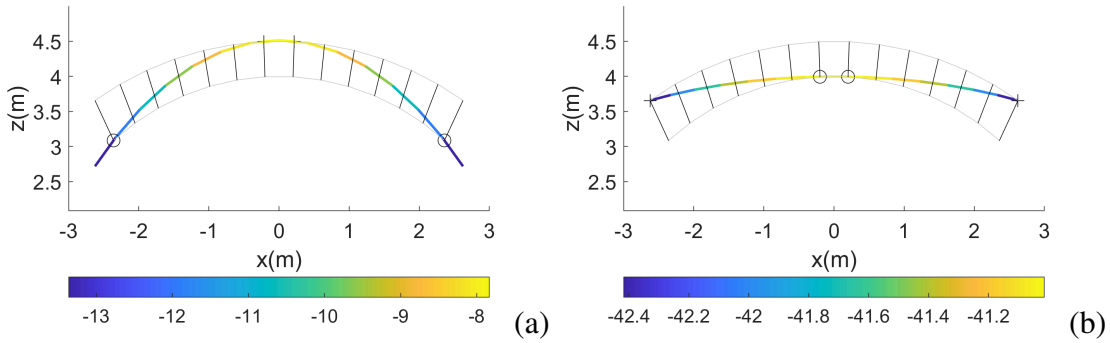

Figure 3: $\sigma_c = -1000\,\text{MPa}$ and infinite friction: (a) min thrust solution ($R_h = 7.795\,\text{kN}$); (b) max thrust solution ($R_h = 41.006\,\text{kN}$).

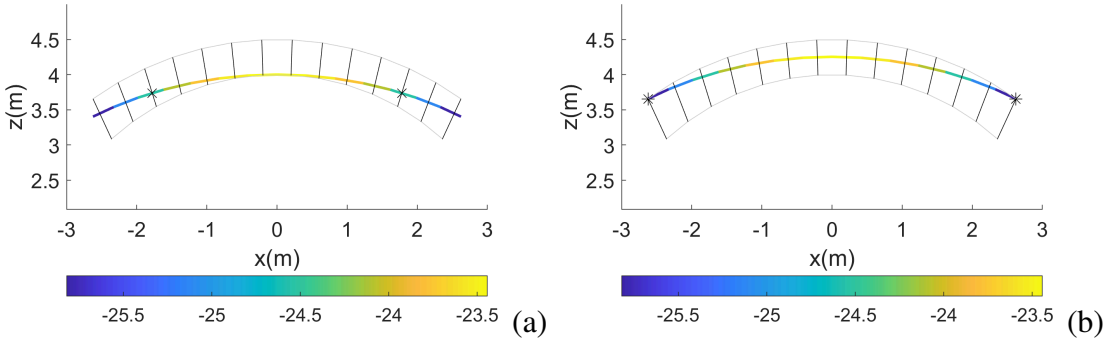

Figure 4: $\sigma_c = -1000\,\text{MPa}$ and $\tan\psi = 0.0004915$: (a) min thrust solution ($R_h = 23.429\,\text{kN}$); (b) max thrust solution ($R_h = 23.429\,\text{kN}$).

tion coefficient a finite value, the limit condition is attained at $\tan\psi = 0.0004915$. In this case, the stability area shrinks to the green segment B_3B_4, corresponding to $f_{min} = f_{max} = 23.427\,\text{kN}$, $-0.0006\,\text{m} \leq e_0 \leq 0.2523\,\text{m}$.

5 Concluding remarks

A numerical procedure based on the constrained force density method is implemented in order to perform the funicular analysis of masonry arches, by taking into account the stereotomy of the voussoirs, as well as a finite value of the friction coefficient. The method is validated by considering a symmetric masonry arch with non-conventional stereotomy. The results obtained through the funicular method are in excellent agreement with those obtained via a modern re-visitation of a classical graphical procedure known as Durand-Claye's method [17, 18], see [16]. A number of analyses have been performed on arches with the same intrados and extrados profiles and different stereotomy, by changing the position of the point from which the joints originate, C_{st}. Such analyses, which will be illustrated more accurately in a forthcoming paper, show that the limit friction coefficient strongly affects the equilibrium of the arch. As a further development of the research, the effects of non-standard behaviour will be ex-

amined, in order to examine more complex typologies of masonry structures, such as non-symmetric masonry arches, vaults and domes.

References

[1] P. Block and J. Ochsendorf, "Thrust network analysis: A new methodology for three-dimensional equilibrium," *J Int Assoc Shell Spat Struct*, vol. 48, no. 155, pp. 167–173, 2007.

[2] P. Block and L. Lachauer, "Three-dimensional funicular analysis of masonry vaults," *Mech Res Commun*, vol. 56, pp. 53–60, 2014.

[3] M. Bruggi, "A constrained force density method for the funicular analysis and design of arches, domes and vaults," *Int J Solids Struct*, vol. 193-194, pp. 251–269, 2020.

[4] J. Heyman, "The stone skeleton," *Int J Solids Struct*, vol. 2, no. 2, pp. 249–279, 1966.

[5] D. Aita, "Between stereotomy and mechanics: joints inclination and minimum thickness in frictionless pointed and circular arches," *Int J Mason Res Innov*, vol. 7, no. 1-2, p. 61 – 88, 2022.

[6] C. Coulomb, "Essai sur une application des règles de maximis et minimis à quelques problèmes de statique, relatifs à l'architecture, mémoires de mathématique et de physique," in *Académie Royale des Sciences par Divers Savans*, pp. 343–382, 1776.

[7] D. Aita, "Between geometry and mechanics: A re-examination of the principles of stereotomy from a statical point of view," in *Proceedings of the first international congress on construction history (Madrid, 20th-24th January 2003)*, vol. 1, pp. 161–170, Instituto Juan de Herrera, 2003.

[8] D. Nikoli? and R. Štuli?, "Equilibrium analysis of frictionless triangular arches: Geometrical formulation," *FME Trans*, vol. 45, no. 2, p. 307 – 313, 2017.

[9] D. Nikolich, "Thrust line analysis of triangular arches," *Archive of Applied Mechanics*, vol. 90, no. 9, p. 1861 – 1874, 2020.

[10] N. Makris and H. Alexakis, "The effect of stereotomy on the shape of the thrust-line and the minimum thickness of semicircular masonry arches," *Arch Appl Mech*, vol. 83, no. 10, p. 1511 – 1533, 2013.

[11] O. Gáspár, A. A. Sipos, and I. Sajtos, "Effect of stereotomy on the lower bound value of minimum thickness of semi-circular masonry arches," *Int J Archit Herit*, vol. 12, no. 6, p. 899 – 921, 2018.

[12] O. Gáspár, I. Sajtos, and A. A. Sipos, "Friction as a geometric constraint on stereotomy in the minimum thickness analysis of circular and elliptical masonry arches," *Int J Solids Struct*, vol. 225, 2021.

[13] M. Fantin and T. Ciblac, "Extension of thrust network analysis with joints consideration and new equilibrium states," *Int J Space Struct*, vol. 31, no. 2-4, pp. 190–202, 2016.

[14] M. Fantin, T. Ciblac, and M. Brocato, "Resistance of flat vaults taking their

stereotomy into account," *J Mech Mater Struct*, vol. 13, no. 5, pp. 657–677, 2018.
[15] C. Casapulla, "Dry rigid block masonry: Safe solutions in presence of coulomb friction," *WIT Transactions on the Built Environment*, vol. 55, pp. 251–261, 2001.
[16] D. Aita, R. Barsotti, and S. Bennati, "Looking at the collapse modes of circular and pointed masonry arches through the lens of durand-claye's stability area method," *Arch Appl Mech*, vol. 89, no. 8, pp. 1537–1554, 2019.
[17] A. Durand-Claye, "Note sur la vérification de la stabilité des voŭtes en maçonnerie et sur l'emploi des courbes de pression," *Ann. Ponts Chaussées*, vol. 13, pp. 63–93, 1867.
[18] A. Durand-Claye, "Note sur la vérification de la stabilité des arcs métalliques et sur l'emploi des courbes de pression," *Ann. Ponts Chaussées*, vol. 15, pp. 109–144, 1867.
[19] H. Schek, "The force density method for form finding and computation of general networks," *Comput Methods Appl Mech Eng*, vol. 3, no. 1, pp. 115–134, 1974.
[20] A. Liew, D. Pagonakis, T. Van Mele, and P. Block, "Load-path optimisation of funicular networks," *Meccanica*, vol. 53, no. 1-2, pp. 279–294, 2018.
[21] M. Bruggi, B. Lógó, and Z. Deák, "Funicular analysis of ribbed masonry vaults: A case study," *Int J Archit Herit*, vol. 16, no. 12, pp. 1809–1823, 2022.
[22] S. Pellegrino and C. R. Calladine, "Matrix analysis of statically and kinematically indeterminate frameworks," *Int J Solids Struct*, vol. 22, no. 4, pp. 409–428, 1986.
[23] D. Aita, R. Barsotti, and S. Bennati, "Equilibrium of pointed, circular, and elliptical masonry arches bearing vertical walls," *J Struct Eng*, vol. 138, no. 7, pp. 880–888, 2012.
[24] K. Svanberg, "The method of moving asymptotes—a new method for structural optimization," *Int J Numer Methods Eng*, vol. 24, no. 2, pp. 359–373, 1987.